Uranium deposits linked to hydrothermal system Formation, evolution, and distribution of uranium through time emphasizing the uranium mineralization linked to hydrothermal system

Sarita Patel*
Solid Earth Research Group, National Centre for Earth Science Studies, Thiruvananthapuram, India
*Corresponding author: sarita29patel@gmail.com

ABSTRACT
This study offers a summary of uranium, highlighting its significance in modern society, as well as its distribution and occurrence in India and globally. Uranium deposits ranging from Neoarchean to Quaternary age are found worldwide, however the well-known economically significant deposits belong to Paleoproterozoic (~1.8 Ga). This study primarily focusses on uranium deposits related to hydrothermal system and explains how geochemical studies of the ore and accessory mineral help to understand the nature, source and physicochemical condition of the mineralizing fluids. A case study on uraninite geochemistry has been performed by compiling the major element data of uraninite from a few hydrothermal uranium deposits. The present dataset and the analyzed plots explain that Pb-concentration is useful in age dating of the uraninite because Pb is the decay product of U. Thus, higher radiogenic Pb suggests older ages and vice versa. Moreover, the incorporation of Th into the uraninite structure is higher at High T hydrothermal system than the Low T system. This study would serve as a preliminary guide for the readers who are interested in research related to uranium mineralization with a specific focus on deposits formed within hydrothermal systems.

ARTICLE HISTORY
Received: 30 November 2025
Revised: 16 December 2025
Accepted: 27 December 2025

KEYWORDS
Uranium
hydrothermal system
uranium deposits
fluids

1. INTRODUCTION
The emergence of nuclear energy in modern days has increased as the world needs an urgent transition from fossil fuels to a carbon free energy source. Such transformation led to a spectacular increase in demand for uranium, the most essential raw material for fueling nuclear reactors. The large-scale global uranium production started after World War II, initially to supply nuclear weapon programs. However, since late 1960s, it switched to the civil nuclear power industry (Mudd and Diesendorf, 2008). The element uranium (U), with atomic number 92 and atomic weight 238, is a silvery-grey metal grouped under the actinide series in the periodic table. It has the second highest atomic weight of the naturally occurring elements, being lighter only than plutonium-244 (^{244}Pu). Uranium has three isotopes i.e., ^{238}U, ^{235}U, and ^{234}U, wherein ^{235}U is naturally fissile, and others are fissionable after interaction with neutrons. The natural abundance of ^{238}U is 99.2745 %, ^{235}U is 0.7200 %, and ^{234}U is 0.0055 %. The half-life of ^{238}U is 4.7 Ga, ^{235}U is 704 Ma, and ^{234}U is 0.245 Ma (Lide, 1995; Steiger and Jäger, 1977). Uranium is a high density metal, denser than lead with a density of 18.9 g/cm3, and has a melting point of 1405 °C. Uranium is a large ion lithophile element (LILE) that can exist in four oxidation states, U^{3+}, U^{4+}, U^{5+}, and U^{6+}, however the most common form found in nature are U^{4+} and U^{6+}, which are also geochemically and mineralogically important. The U^{4+} occurs in subsurface environments, while U^{6+} is stable under oxidizing conditions. Uranium preferably enters into the lattices of the accessory minerals and is highly incompatible to most of the rock-forming minerals (Brooks and Kelly, 1983; Dahlkamp, 1993; Hoffman et al., 1971). As an incompatible element it is strongly concentrated in the Earth's crust (0.26–1.8ppm) than the mantle (0.13ppm in the undepleted mantle to 0.032ppm in the present mantle). The oxidation state plays major control in uranium geochemistry. In oxidizing fluids, uranium transports as the hexavalent uranyl ion (UO_2^{2+}), whereas in reducing environments, it precipitates as $U^{4+}O_2$. Precipitation of uranium in most ore

deposits is related to a decrease of fO_2, generally resulting from the interaction of oxidized U-bearing fluids with carbonaceous materials such as anaerobic bacteria/ graphite. Other potential reductants are H_2S, magnetite, ilmenite, and sulfides (Brookins, 1978; Cuney, 2009; Hamilton, 1975; Rich et al., 1977; Szalay and Samsoni, 1969). This study reviews the evolutionary history of uranium through time, classification of the uranium deposits based on the geological environments (host rocks, and tectonic settings), and genetic processes (source, transport, concentration). Then a small case study is included to understand the uranium deposits linked to hydrothermal system.

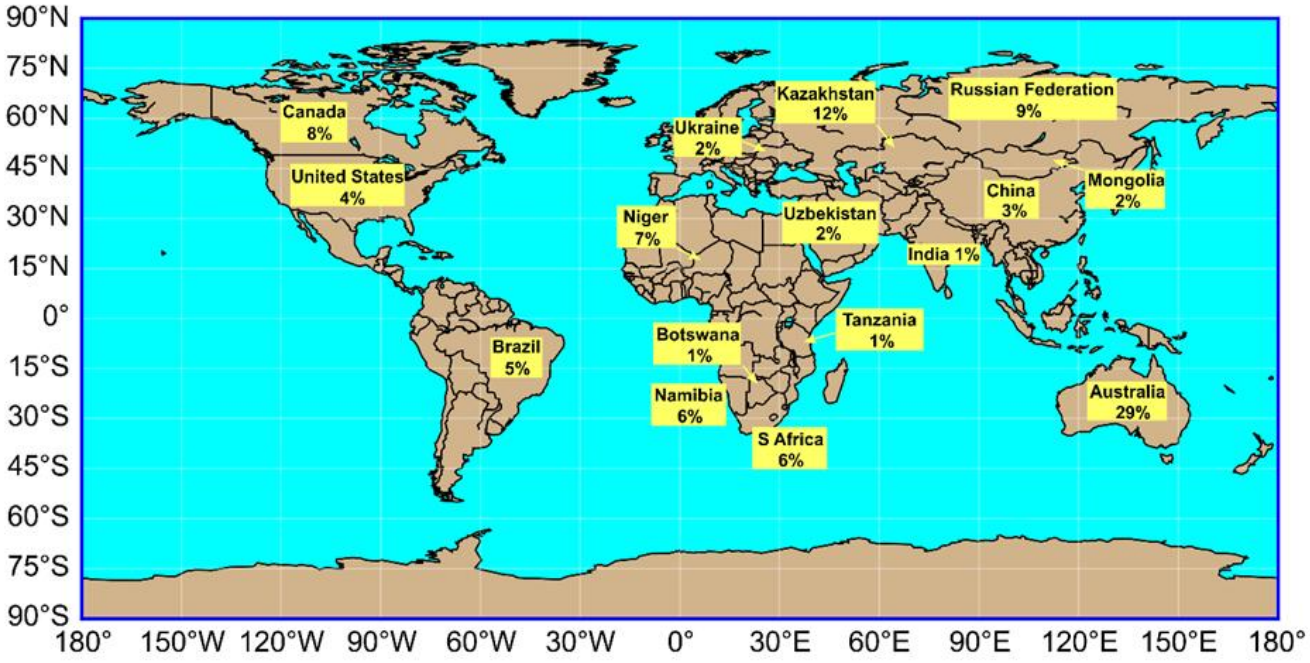

Figure 1. Global distribution of identified resources of uranium with more than a 1% share of the total global identified resources available at costs <USD 130/kgU (modified after the joint report by the OECD Nuclear Energy Agency and the International Atomic Energy Agency).

2. DISTRIBUTION OF URANIUM WITH CRUSTAL EVOLUTION

Uranium deposits exist almost in all continents (Fig. 1) and have formed over a protracted geological period from Neoarchean to Quaternary. The evolution of the uranium fractionation process through time led to the formation of global uranium deposits that are grouped below in different time interval for clarity and ease of understanding, and this grouping is after Cuney (2010).

(i) The Hadean to Paleoarchean interval (ca. 4.55–3.20 Ga) involves the formation of the most fractionated trondhjemite-tonalite-granodiorite (TTG) rocks, wherein the refractory accessory minerals attained uranium concentrations of a few parts per million.

(ii) The Paleoarchean to Mesoarchean interval (ca. 3.8 to 3.3 Ga), generation of sodium-rich magmas introduced the first notable quantity of radioelements into the crust. This period marks the complete absence of free oxygen. Thus, no uranium deposit was expected to form during this period.

(iii) The Neoarchean–Paleoproterozoic interval (ca. 3.1 to 2.2 Ga), introduction of several extensive pulses of highly fractionated potassic granites significantly enriched in U, Th, and K into the earth crust. Two major phenomena characterize this interval:

a. At ca. 2.8–2.4 Ga: formation of K-rich granitic/pegmatitic magmas that led to enrichment of the radioactive elements in granitic rocks. These uranium-bearing granitic complexes became the source for subsequent uranium recycling in different parts of the world, such as the Yilgarn Block, Australia; Superior Province, Canada; Kaapvaal/Kalahari Craton, South Africa; Sao Francisco Craton, Brazil.

b. At ca. 2.4–2.2 Ga: formation of the major intra-cratonic basins for the first time after cratonization. These basins accumulated clastic sediments, primarily arenites, including oligomictic quartz-pebble conglomerates, which gathered significant amounts of detrital uraninite and other heavy minerals. Such continental basins with uranium reserves throughout the world are present in the Huronian Blind River-Elliot Lake-Quirke Lake Basin, Canada; Witwatersrand Basin, South Africa; Serra de Jacobina and Quadrilatero Ferrifero, Brazil; Nullagine Conglomerate, Australia; Palimba Conglomerate, Jenissei province, Russia. The scarcity of free oxygen during this period prevented the oxidation of the uraninite, which produced the Earth's earliest economic uranium deposit types. However, the occurrence of Paleoproterozoic banded iron formations at the time of uranium-bearing conglomerate deposition can sometimes contradict the anoxic atmosphere. On the other hand, Schidlowski et al. (1975) argued that the first oxygen formed in seawater by photosynthesis of early life forms (green algae). This oxygen was used to oxidize reduced compounds, particularly ferrous iron, in the oceans for a long time. Consequently, banded iron formation precipitated in the marine basins where oxygen generation was early or more advanced, whereas the uraninite placers accumulated in the concomitant intra-cratonic basins.

(iv) The Paleoproterozoic–Tertiary interval (from 2.2 to 0.45 Ga), records a surge in oxygen up to the present atmospheric level, development of sedimentary basins, and marine microorganisms (algae). During late Paleoproterozoic, tetravalent uranium from uraninite, trapped in reduced epicontinental sedimentary successions containing organic matter and phosphates, was oxidized to hexavalent uranium and formed highly soluble uranyl ions in water. Redox processes gave rise to a sequence of uranium deposits, the first of which appeared at 2.0 Ga in the Oklo area of Gabon. All known economically significant uranium deposits related to Na metasomatism are of ca. 1.8 Ga age. Unconformity related to high grade deposits and with significantly high tonnage originated primarily during the time interval from late Paleoproterozoic to early Mesoproterozoic. Some important deposits of this period include Beaverlodge, Athabasca, Kaipokok Bay - Big River districts, Canada; Alligator Rivers, Rum Jungle districts, Australia; Pan-African and Brazilian mobile belts, Africa, South America; Singhbhum Shear Zone, India; Arjeplog-Arvidsjaur province, Sweden; South Greenland province, Greenland; and Krivoy Rog, Ukraine.

(v) The Tertiary–Present interval (i.e., 0.45 Ga to present), intra-formational reduction traps developed by plant detritus accumulating within continental siliciclastic strata during the late phase of uranium deposits. During this time, basal, roll front, tabular, and tectono-lithologic deposits formed, such as the Colorado Plateau, Wyoming Basins, South Texas Coastal Plains, USA; Lake Frome Embayment, Australia; Agades Basin, Niger; Parana Basin, Brazil; North Bohemian Basin, CSFR Germany; Kyzylkumsky, Uzbekistan; Jingan Basin, China. In summary, the evolution of the global uranium deposits is controlled by the following factors: (1) major changes in tectonic conditions during Neoarchean, (2) striking increase in atmospheric oxygen between 2.4 and 2.2 Ga, and (3) development of land plants during the Silurian (Cuney, 2009, 2010; Dahlkamp, 1993).

3. CLASSIFICATION OF URANIUM DEPOSITS

The uranium deposits are classified based on the host rock and the ore localizing structures with which they are associated. This geological classification of uranium deposits was made by the IAEA (International Atomic Energy Agency), which has published guidebooks on the world distribution of uranium deposits since 1996. A deposit must have minimum resources of > 500 t U at an average of 0.03 % U or greater to be included in the IAEA database.

As of December 2017, the IAEA database includes 2939 deposits distributed amongst 15 types, 38 subtypes, and 14 classes (Bruneton et al., 2018). These 15 types are given in Table 1.

Table 1. Classification of the uranium deposits based on IAEA database (Bruneton et al., 2018).

Types	Description of U-deposit	No. of deposits	Volume	Description
Type 1	Intrusive type	129	2,847,000t U	Associated with rocks like alaskite, granite, and pegmatite (e.g., Rössing, Namibia).
Type 2	Granite related	586	527,000t U	Granite-related deposits or vein-type deposits are hydrothermal uranium deposits which has genetic relationship to granitic intrusions. (e.g., Nanling Metallogenic Belt, South China, Bohemian massif, Central Europe, Beaverlodge District, Canada)
Type 3	Polymetallic iron oxide breccia complex (IOCG)	21	2,562,500t U	Large, low-grade deposits where uranium is often a by-product (e.g., Olympic Dam, Australia—the world's largest uranium resource).
Type 4	Volcanic related	204	1,908,500t U	Occur in or near volcanic calderas in felsic rocks (e.g., Streltsovskoye, Russia).
Type 5	Metasomatite	152	1,070,000t U	Formed by intense sodium or potassium metasomatism in structurally deformed rocks (e.g., Lagoa Real, Brazil).
Type 6	Metamorphite	225	663,000t U	Occurs in metasediments or metavolcanics unrelated to granites (e.g., Mary Kathleen, Australia).
Type 7	Proterozoic unconformity	114	1,547,500t U	High-grade deposits located near the contact between Proterozoic sandstone and older metamorphic basement (e.g., McArthur River, Canada).
Type 8	Collapse breccia pipe	18	19,500t U	Vertical, circular structures filled with sediment fragments (e.g., Arizona Strip, USA).
Type 9	Sandstone-hosted	951	4,827,000t U	The most common type globally. Uranium precipitates under reducing conditions in porous sandstone. Major subtypes include: Roll front: Crescent-shaped bodies (e.g., Inkai, Kazakhstan). Tabular: Lenticular bodies parallel to bedding (e.g., Akouta, Niger).
Type 10	Paleo-quartz-pebble conglomerate	144	2,504,000t U	Detrital uranium in ancient conglomerates (e.g., Witwatersrand, South Africa).
Type 11	Surficial	123	532,000t U	Near-surface concentrations in sediments or soils, often cemented by calcrete in arid regions (e.g., Yeelirrie, Australia).
Type 12	Lignite-coal	75	7,406,500t U	Uranium adsorbed onto organic matter in coal or lignite beds.
Type 13	Carbonate	34	184,000t U	Deposits hosted in limestone or dolomite
Type 14	Phosphate associated	73	14,326,000t U	Marine phosphorites containing trace amounts of uranium as a by-product.
Type 15	Black shale	75	21,749,000t U	Large, very low-grade marine organic-rich shales (e.g., Ranstad, Sweden).

Amongst the deposits mentioned in Table 1, the largest resources are present in unconventional resource deposit types such as those associated with polymetallic iron oxide breccia complex (IOCG-U), phosphate, lignite–coal, and black shale. In the IOCG type uranium deposits, 80% of the resources are in the Olympic Dam deposit, Australia. Sandstone-hosted uranium deposits are the conventional resource deposit types, followed by Proterozoic unconformity and volcanic-related deposit types. Uranium deposits related to hydrothermal processes are typically epigenetic (Bruneton et al., 2018; Cuney, 2009). In modern geology, "hydrothermal uranium deposits/ uranium deposits linked to hydrothermal system" is an umbrella term for mineral systems where uranium is concentrated by circulating hot fluids (50 °C to > 400 °C) (Romberger, 1984; Timofeev et al., 2018). For example, the uranium

mineralization in the SSZ, India is very close to metamorphite and metasomatite types based on the temperature and nature of formation. However, the overall mineralization along the Singhbhum Shear Zone (SSZ) is polymetallic (Cu, Au, U, Fe, Co, Mo, REE), it is affected by multiple episodes of hydrothermal activities and sodium metasomatism, the mineralizing fluids are saline, high temperature, and acidic that group it into IOCG(U-REE) type mineralization (Pal et al., 2023, 2010, 2009; Patel et al., 2023, 2021).

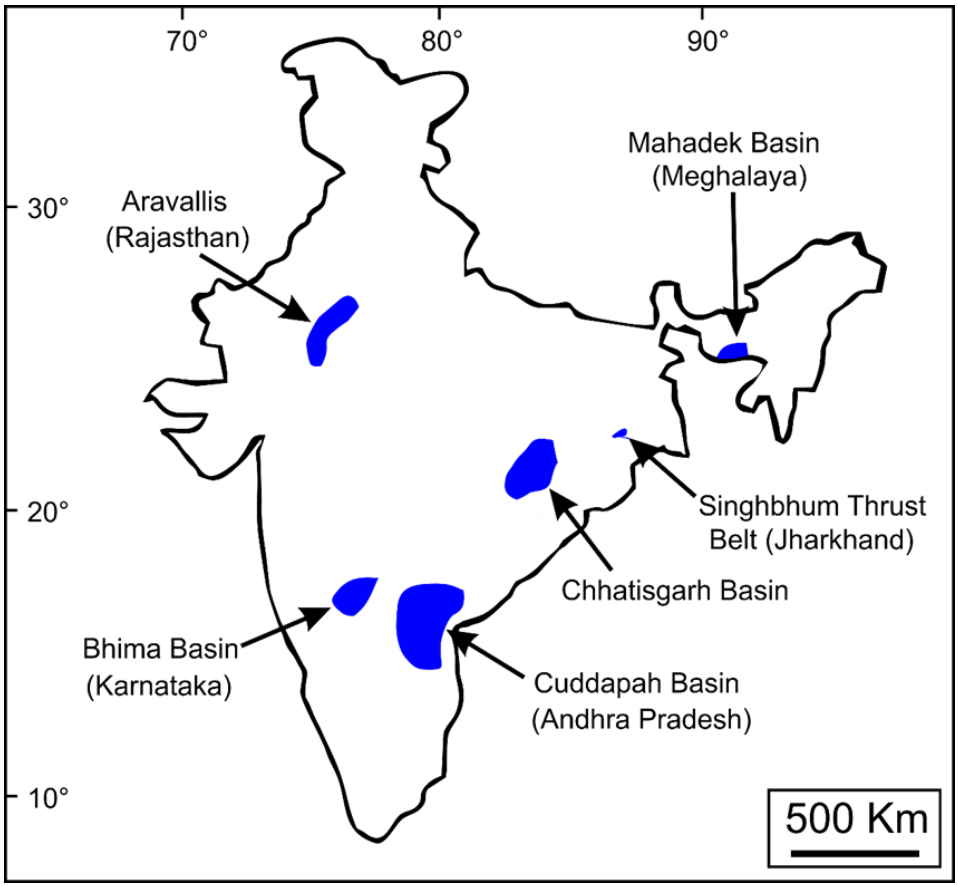

Figure 2. Location of uranium occurrences in in India (Gupta and Sarangi, 2005).

4. URANIUM DEPOSITS IN INDIA

The atomic energy program of India commenced in 1948 with the establishment of the Atomic Energy Commission. Therefore, the Indian government established a Rare Metal Survey Unit, subsequently renamed as the Atomic Minerals Directorate for Exploration and Research, to discover uranium reserves within the nation. The country's first uranium deposit was discovered in 1951 in the Singhbhum Shear Zone (SSZ), in the state of Jharkhand (Fig. 2). In this belt, Jaduguda was the initial site for extensive exploration and extraction, followed by discovery of other mines such as Bhatin, Narwapahar, Turamdih, Bagjata, Banduhurang, and Mohuldih. Garadih, Kanyaluka, Nimdih, and Nandup constitutes the prospects that have modest reserves with substandard grades (Gupta and Sarangi, 2005). As per the IAEA's revised geological classification of uranium deposits in 2013, the Jaduguda uranium deposit of SSZ, India, is grouped under polymetallic metamorphite type uranium deposit in Bruneton et al. (2014), while the recent research provides strong evidence for it to be IOCG (U-REE) type (Pal et al., 2023; Patel et al., 2023, 2021). Uranium potential has predominantly been identified in the Cuddapah basin of Andhra Pradesh, India (Fig. 2). Locations such as Lambapur-Peddagattu, Chitrial, Kuppunuru, Tumallapalle, and Rachakuntapalle have significantly contributed to India's uranium reserve base, with Tumallapalle being the most significant one. The deposits in this region are situated at the unconformity contacts of underlying granites and overlying quartzites. Sandstone type

uranium deposits have been identified in the Mahadek basin of Meghalaya in the North-Eastern part of India (Fig. 2), namely in Domiasiat, Wahkhyn, and Mawsynram. They provide near-surface, flat orebodies suitable for open-pit mining operations. Other regions of Rajasthan, Karnataka, and Chhattisgarh possess the potential to evolve into large deposits (Gupta and Sarangi, 2005).

5. PROCESSES OF FORMATION OF HYDROTHERMAL URANIUM DEPOSITS

The formation of hydrothermal uranium deposits is a multi-stage process involving the leaching, transport, and precipitation of uranium by hydrothermal fluids. These processes are controlled by geology, tectonic activity, and the physicochemical conditions of the region (Cuney and Kyser, 2009; Romberger, 1984). The stages are explained below in detail and through the schematic illustration in figure 3.

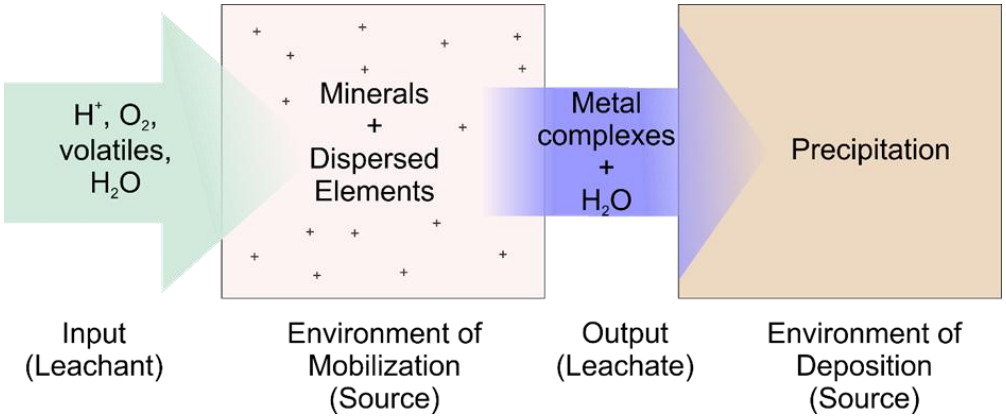

Figure 3. Schematic representation of environment of uranium mineralization (modified after Romberger, 1984).

5.1 Source and mobilization

Mineralizing solutions derived from various sources including magmatic, connate, or meteoric (surface) water, circulate through the source rocks, effectively leaching the uranium (Fig. 3). Uranium and associated metals are derived from the granitic rocks as U is a common trace element in the accessory minerals like apatite and monazite. The uranium-bearing fluids migrate through zones of weakness, such as faults, fractures, and shear zones in the Earth's crust (Cuney and Kyser, 2009; Hughes and Rakovan, 2015; Romberger, 1984).

5.2 Transportation

In general, uranium is transported in the U^{6+} oxidation state and is insoluble in the U^{4+} state (Romberger, 1984). The properties like porosity and permeability of the host rock are crucial in channeling these fluids and localizing the deposition process. Furthermore, solubility of uranium is highly dependent on the fluid's chemical conditions, including temperature, pressure, pH, and oxygen levels (Eh), and complexation. Solubility of uranium in acidic F-rich hydrothermal fluids in the form of $U^{+4}F$ complexes in reducing condition and uranyl $(UO_2^{2+})F$ complexes in oxidizing condition predominate at low temperature, while uranyl chloride (such as UO_2Cl_2) complexes predominate at temperature > 150 °C. In hydrothermal system the ideal condition for U transportation is high temperature (> 150 °C), Cl-rich, and highly acidic fluids and the reverse is favorable for precipitation. Important uranyl complexes in acidic solution are UO_2Cl_2 and $UO_2(OH)_2$. At low temperatures and in alkaline solutions carbonate complexation predominates, while at ≥300 °C hydroxide complexes become the only soluble uranium species (Migdisov et al., 2018; Romberger, 1984; Timofeev et al., 2018; Xing et al., 2018). Presence of phosphate minerals such as apatite in a hydrothermal system indicates that high phosphate activity could lead to the transportation of uranium as phosphate complexes (Jiménez-Arroyo et al., 2023).

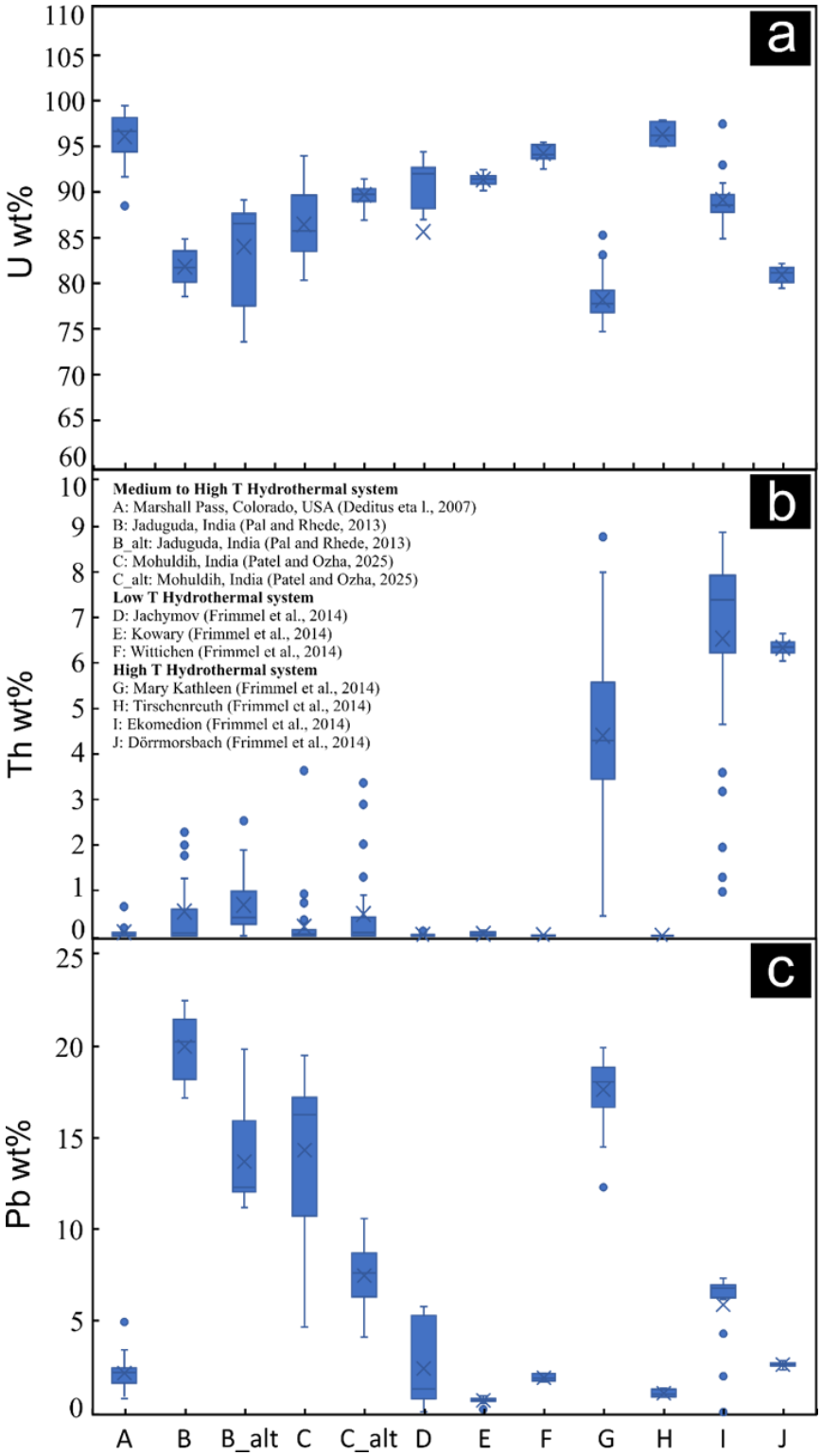

Figure 4. Box and whisker plots of U, Th, and Pb (in wt%) illustrate the distribution of these elements throughout several deposits associated with distinct hydrothermal systems based on temperature. The plot displays that U and Pb concentration in uraninite are linked i.e., the uraninite with high U have low Pb concentration and vice versa (Fig. a, c). The uraninites from Low temperature and Medium to High temperature hydrothermal system have low Th concentration than the uraninites from High temperature hydrothermal system.

5.3 Deposition

Deposition/precipitation of uranium would be promoted by reduction and/or increase in pH of the transporting solutions, which causes the dissolved, oxidized U^{6+} to be reduced to insoluble U^{4+}, forming minerals like pitchblende or uraninite. Concentration of uranium that led to an ore body in a hydrothermal system occur via cavity filling of fractures/veins and metasomatic replacement of the host rocks. The chemical changes observed in rocks that have undergone hydrothermal alteration reveal the history of fluid-rock interactions, providing key geochemical indicators used to pinpoint mineralized sites. Furthermore, reducing agents such as organic matter, hydrocarbons, or iron-bearing minerals like pyrite or chlorite in the host rock plays an important role for uranium precipitation (Li et al., 2024; Romberger, 1984; Spirakis, 1996). Sulfate is a powerful oxidizing agent at high-temperature water, but as the solution cools to around 200 °C, the chemical reactions involving sulfate slow down. This kinetic effect reduces sulfate's ability to act as an oxidizing agent. Consequently, the reducing capacity of other substances like H_2S is no longer fully balanced by sulfate's oxidizing effect, making the entire solution more reducing as it cools. This shift in conditions is exactly what is necessary for the precipitation of reduced uranium minerals to form ore deposits, a process that may also occur in other types of epithermal deposits (Spirakis, 1981).

A recent study using geochemical modeling by Moore et al. (2024) explains how the evolutionary history of Earth has impacted the global uranium cycle, evolving uranium mineral chemistry, and deposit formation through time. The results illustrate the following (1) the common uranium mineral uraninite (UO_2), which form in anoxic condition were abundant in the Archean eon than present day oxic conditions. (2) Uranium minerals are increasingly oxidized through time that result new minerals with diversifying chemical element associations and expanding distribution of uranium in the environment. (3) The increase in the number of oxidized U^{6+} uranium minerals in sedimentary environment than reduced U^{4+} uranium minerals started at around ca. 350–250 Ma that represent the evolution of continental weathering with Earth surface oxidation, the development of land plants and redox-controlled U deposition from ground water in continental sediments during this time-period. Furthermore, the experimental results of Timofeev et al. (2018) explains that uranium can also be mobile in reducing condition (U^{+4} state) in the form of UCl_4^0 complex at high temperature (~250–350 °C).

6. FLUID PROXIES AND GEOCHRONOMETERS USED FOR RESEARCH ON URANIUM ORE GENESIS

The current importance and need for uranium encourage research on uranium ore genesis. Establishing the source of the mineralizing fluid and its evolution during fluid-rock interaction is essential for formulating ore genetic models for hydrothermal ore deposits. Several proxies such as fluid inclusions, stable isotopes (of oxygen, hydrogen, carbon, sulfur, nitrogen, and boron), and the composition of hydrothermally precipitated ore and gangue (such as tourmaline, magnetite, and apatite) minerals have been used to trace the source and evolution of ore forming fluids in hydrothermal deposits (Hoefs, 2009; Ohmoto and Goldhaber, 1997; Ridley, 2013; Roedder and Bodnar, 1997; Taylor, 1997). Timing of mineralization is a crucial parameter for comprehensive understanding of hydrothermal ore deposits. Therefore, we need to look for minerals that accommodate appreciable quantities of U, Th and Pb in their crystal structures. Some of the well-known and commonly used chronometers are zircon (Kerrich and King, 1993), monazite (Aleinikoff et al., 2012; Muhling et al., 2012; Rasmussen et al., 2010, 2007; Vielreicher et al., 2010), allanite (Boston et al., 2017; Darling et al., 2012; Gieré and Sorensen, 2004; Janots et al., 2009; Wing et al., 2003; Wood and Ricketts, 2000), xenotime (Vielreicher et al., 2003), titanite (e.g., Lin and Corfu, 2002), and rutile (e.g., Zack et al., 2011).

7. REVEALING THE NATURE AND EVOLUTION OF THE FLUID FROM URANINITE GEOCHEMISTRY WITH SOME GLOBAL EXAMPLE

The important ore minerals of uranium are uraninite (UO_2), coffinite ($U(SiO_4)_{1-x}(OH)_{4x}$), brannerite (UTi_2O_6), davidite [(REE) (Y, U) (Ti, Fe^{3+})$_{20}O_{38}$], and thucholite (uranium-bearing pyrobitumen). Amongst these, uraninite with U-content (up to 88.2 wt. % U) is the most abundant U^{4+} mineral in nature. Pure uraninite ($U^{4+}O_2$) is very

rare due to auto-oxidation caused by radioactive decay of uranium and non-stoichiometry (Finch and Murakami, 1999; Janeczek and Ewing, 1992; Smith, 1984). The ^{238}U, and ^{235}U isotopes of uranium decay to ^{206}Pb and ^{207}Pb, respectively, which is the reason for variable amounts of radiogenic lead in the structure of uraninite. Impurities like Pb, Th, rare earth elements (REE), and Ca may incorporate into the interstitial sites of UO_{2+x}. The structural formula of thorium-absent uraninite is $(U^{4+}_{1-x-y-z}U^{6+}_{x}REE^{3+}_{y}M^{2+}_{z})\ O_{2+x-0.5y-z}$, where M predominantly stands divalent cations such as Pb and Ca (Finch and Murakami, 1999; Janeczek and Ewing, 1992). The amount of trace (REE and Y) and minor elements (Si, Ca, Fe, Al, K, Ti, and Na) within uraninite is a function of the temperature, redox state, and fluid composition prevalent during uraninite formation (Alexandre and Kyser, 2005; Eglinger et al., 2013; Mercadier et al., 2011; Pal and Rhede, 2013). The concentrations of other elements in uraninite can act as geochemical tracers and help to chemically constrain its environment of formation. Geochemical characterization, in conjunction with in-situ dating of uraninite, can limit the timing of mineralization and subsequent alteration, if any. The concentration of Pb (all measured Pb are considered to be radiogenic) is useful in "chemical dating" of uraninite, especially the variations that occur within the oscillatory zoning that can be used to infer the composition of altering fluids (Alexandre and Kyser, 2005; Deditius et al., 2007; Kempe, 2003; Pal and Rhede, 2013).

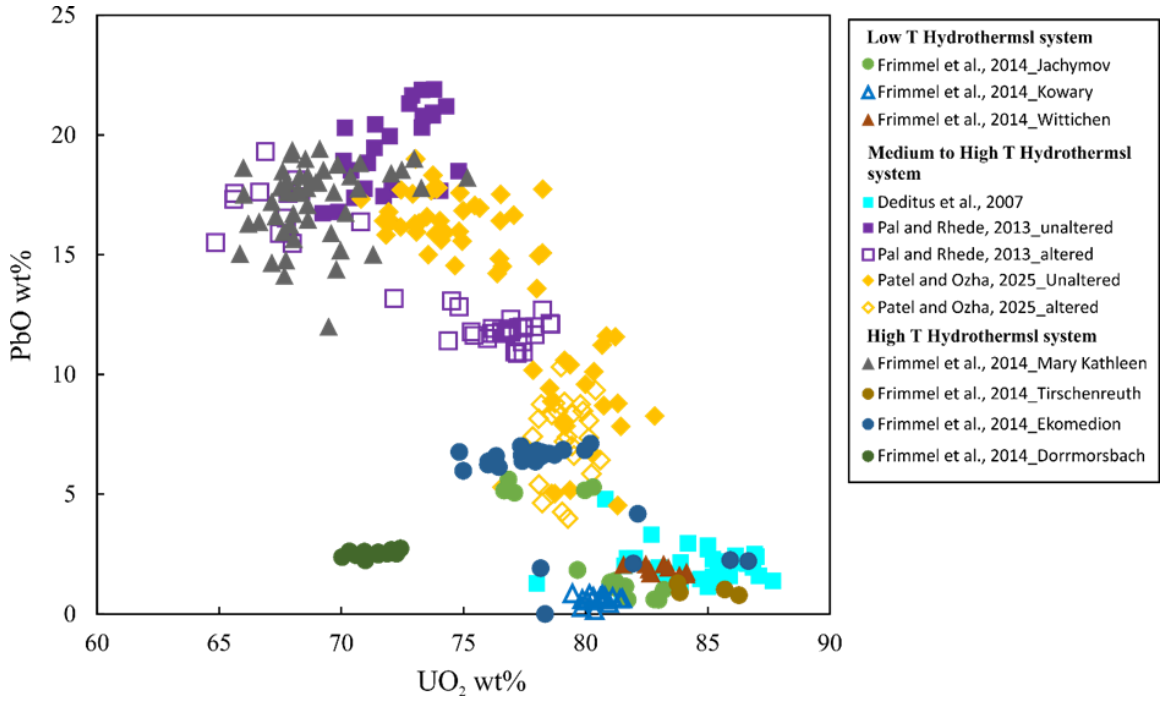

Figure 5. Bivariate plots between UO_2 and PbO (in wt%) content in uraninite from different hydrothermal systems. The plot displays a strong negative correlation between UO_2 and PbO, where the unaltered uraninite have relatively high PbO concentration than the altered uraninite.

In the present study, the major elements data of uraninite is curated from a few important hydrothermal uranium deposits (Supplementary Table 1) as a case study purpose. The deposits are grouped into three groups based on temperature such as (i) Medium to High T hydrothermal system, (2) Low-T hydrothermal system, and (3) High T hydrothermal system. The boxplots of U and Pb concentration (Fig. 4a and c) present that the uraninite with higher U content have lower Pb content and vice versa. The higher content of Pb in uraninite grains are most probably the radiogenic Pb due to decay of U. However, less Pb content may indicate less radiogenic Pb that suggests the uraninite are relatively younger in time than the former. This can be further checked from Pal and Rhede (2013) and Patel and Ozha (2025) uraninite data, where age of the uraninites is also calculated by chemical dating method. In the above-mentioned publications uraninite grains are grouped into unaltered uraninite (remnants of the uraninite formed during primary hydrothermal event) and altered uraninite (freshly formed uraninite during later hydrothermal

events). In the bivariate plot between UO_2 (in wt%) and PbO (in wt%), (Fig. 5) the unaltered uraninite have relatively high PbO and low UO_2 content than the altered uraninite suggests that the former is older than the later. Hence, we can interpret from figure 5 that the uraninite from all the other locations of Frimmel et al. (2014) except Mary Kathleen are younger in age because they have high UO_2 and low PbO concentration. The box plot (Fig. 4b) suggests that the uraninite from the High T hydrothermal systems have higher Th concentration followed by Medium to High T and then Low T systems. This suggests the Th uptake in the structure of uraninite is controlled by temperature. Thus, Th content in uraninite serves as an indicator for distinguishing granite/pegmatite-derived uraninite from low-temperature, hydrothermal uraninite (Bea, 1996; Grandstaff, 1981). Here, only the U, Th, and Pb concentration of uraninite are discussed, whereas other major elements, trace elements, and REEs are also used now-a-days for ore genetic studies i.e., to understand the deposit and the evolutionary history in detail.

8. CONCLUSIONS

Conventional hypothesis suggests that uranium is transported in oxidizing (in the form of U^{+6}) condition and precipitates in reducing condition (in U^{+4} state), while the modern research has experimentally proved that at certain conditions and environment uranium can be mobile in U^{+4} state also. Moreover, in modern times there is increase in the formation of oxidized U^{6+} uranium minerals than the uraninite (UO_2), which formed in anoxic condition during the Archean eon. The case study presented in the present work shows that U and Pb concentration in uraninite are controlled by time such as the older uraninites have higher radiogenic Pb and low U concentration, while the younger uraninite have high U concentration and low radiogenic Pb. Thorium concentration in uraninite is temperature dependent i.e., it is high in high T and low in low T. Uraninite/any U-bearing mineral geochemistry is important for mineral exploration and also in the assessment of the quality of the mineral.

Supplementary Table

Supplementary Table 1: Major element data of uraninite taken from a few well-known hydrothermal uranium deposits across the world.

References

Aleinikoff, J.N., Slack, J.F., Lund, K., Evans, K. V, Fanning, C.M., Mazdab, F.K., Wooden, J.L. and Pillers, R.M. (2012). Constraints on the timing of Co-Cu±Au mineralization in the Blackbird district, Idaho, using SHRIMP U-Pb ages of monazite and xenotime plus zircon ages of related Mesoproterozoic orthogneisses and metasedimentary rocks. Econ. Geol., 107, pp.1143–1175

Alexandre, P. and Kyser, T.K. (2005). Effects of cationic substitutions and alteration in uraninite, and implications for the dating of uranium deposits. Can. Mineral., 43, pp.1005–1017

Bea, F. (1996). Residence of REE, Y, Th and U in granites and crustal protoliths; implications for the chemistry of crustal melts. J. Petrol., 37, pp.521–552

Boston, K.R., Rubatto, D., Hermann, J., Engi, M. and Amelin, Y. (2017). Geochronology of accessory allanite and monazite in the Barrovian metamorphic sequence of the Central Alps, Switzerland. Lithos, 286–287, pp.502–518

Brooks, M.S.S. and Kelly, P.J. (1983). On the cohesive energy and charge density of uranium dioxide. Solid State Commun., 45, pp.689–692

Bruneton, P., Cuney, M., Dahlkamp, F. and Zaluski, G. (2014). IAEA geological classification of uranium deposits, in: In: International symposium on uranium raw material for the nuclear fuel cycle, Austria, pp.12–13

Bruneton, P., Cuney, M., Fairclough, M., Jaireth, S., Liu, X. and Zaluski, G. (2018). UDEPO: The IAEA Uranium Deposits Database.

Cuney, M. (2010). Evolution of Uranium Fractionation Processes through Time: Driving the Secular Variation of Uranium Deposit Types. Econ. Geol., 105, pp.553–569

Cuney, M. (2009). The extreme diversity of uranium deposits. Miner. Depos., 44, pp.3–9

Cuney, M. and Kyser, K. (2009). Hydrothermal uranium deposits related to igneous rocks. In: Recent and not-so-recent developments in uranium deposits and implications for exploration (eds. M. Cuney and K. Kyser). Mineralogical Association of Canada, Short Course Series, 39, Quebec, pp.119–162

Dahlkamp, F.J. (1993). Geology of the uranium deposits. Springer.

Darling, J.R., Storey, C.D. and Engi, M. (2012). Allanite U–Th–Pb geochronology by laser ablation ICPMS. Chem. Geol., 292, pp.103–115

Deditius, A.P., Utsunomiya, S. and Ewing, R.C. (2007). Fate of trace elements during alteration of uraninite in a hydrothermal vein-type U-deposit from Marshall Pass, Colorado, USA. Geochim. Cosmochim. Acta, 71, pp.4954–4973

Eglinger, A., André-Mayer, A.-S., Vanderhaeghe, O., Mercadier, J., Cuney, M., Decrée, S., Feybesse, J.-L. and Milesi, J.-P. (2013). Geochemical signatures of uranium oxides in the Lufilian belt: From unconformity-related to syn-metamorphic uranium deposits during the Pan-African orogenic cycle. Ore Geol. Rev., 54, pp.197–213

Ferguson, J. (1988). The uranium cycle. IAEA, International Atomic Energy Agency (IAEA).

Finch, R. and Murakami, T. (1999). Systematics and paragenesis of uranium minerals. In: Uranium: Mineralogy, Geochemistry and the Environment, P.C. Burns, R. Finch (Eds.), Reviews in Mineralogy, 38, Mineralogical Society of America, Washington, DC (1999), pp.91-179

Frimmel, H.E., Schedel, S. and Brätz, H. (2014). Uraninite chemistry as forensic tool for provenance analysis. Appl. Geochemistry, 48, pp.104–121

Gieré, R. and Sorensen, S.S. (2004). Allanite and Other REE-Rich Epidote-Group Minerals. Rev. Mineral. Geochemistry, 56, pp.431–493

Grandstaff, D.E. (1981). Uraninite oxidation and the Precambrian atmosphere. USGS-PP-1161-A-BB

Gupta, R. and Sarangi, A.K. (2005). Emerging trend of Uranium mining: the Indian scenario. In: IAEA International Symposium on" Uranium Production and Raw Materials for the Nuclear Fuel Cycle-Supply and Demand, Economics, the Environment and Energy Security", Vienna. pp.47–56

Hamilton, E.I. (1975). The abundance and distribution of uranium in some oceanic, continental ultramafic inclusions and host basalts. Chem. Geol., 16, pp.221–231

Hoefs, J. (2009). Stable isotope geochemistry, 6th ed. Springer Berlin.

Hoffman, D.C., Lawrence, F.O., Mewherter, J.L. and Rourke, F.M. (1971). Detection of Plutonium-244 in Nature. Nature, 234, pp.132–134

Hughes, J.M. and Rakovan, J.F. (2015). Structurally Robust, Chemically Diverse: Apatite and Apatite Supergroup Minerals. Elements, 11, pp.165–170

Janeczek, J. and Ewing, R.C. (1992). Structural formula of uraninite. J. Nucl. Mater., 190, pp.128–132

Janots, E., Engi, M., Rubatto, D., Berger, A., Gregory, C. and Rahn, M. (2009). Metamorphic rates in collisional orogeny from in situ allanite and monazite dating. Geology, 37, pp.11–14

Jiménez-Arroyo, Á., Gabitov, R., Migdisov, A., Lui, J., Strzelecki, A., Zhao, X., Guo, X., Paul, V., Mlsna, T., Perez-Huerta, A., Caporuscio, F., Xu, H. and Roback, R. (2023). Uranium uptake by phosphate minerals at hydrothermal conditions. Chem. Geol., 634, p.121581

Kempe, U. (2003). Precise electron microprobe age determination in altered uraninite: consequences on the intrusion age and the metallogenic significance of the Kirchberg granite (Erzgebirge, Germany). Contrib. to Mineral. Petrol., 145, pp.107–118

Kerrich, R. and King, R. (1993). Hydrothermal zircon and baddeleyite in Val-d'Or Archean mesothermal gold deposits: characteristics, compositions, and fluid-inclusion properties, with implications for timing of primary gold mineralization. Can. J. Earth Sci., 30, pp.2334–2351

Li, F.-R., Zhang, Y., Dang, F.-P., Huang, D., Zhong, F.-J., Yan, J., Xia, F., Pan, C.-R., Pan, J.-Y., Han, S.-C., Liu, G.-Q., Zhang, X.-T., Liu, Y. and Wang, K.-X. (2024). The role of hydrothermal alteration in uranium mineralization at the Xiaoshan uranium deposit, South China. Ore Geol. Rev., 174, p.106324

Lide, D.R. (1995). CRC handbook of chemistry and physics: a ready-reference book of chemical and physical data. CRC press.

Lin, S. and Corfu, F. (2002). Structural Setting and Geochronology of Auriferous Quartz Veins at the High Rock Island Gold Deposit, Northwestern Superior Province, Manitoba, Canada. Econ. Geol., 97, pp.43–57

Mercadier, J., Cuney, M., Lach, P., Boiron, M., Bonhoure, J., Richard, A., Leisen, M. and Kister, P. (2011). Origin of uranium deposits revealed by their rare earth element signature. Terra Nova, 23, pp.264–269

Migdisov, A.A., Boukhalfa, H., Timofeev, A., Runde, W., Roback, R. and Williams-Jones, A.E. (2018). A spectroscopic study of uranyl speciation in chloride-bearing solutions at temperatures up to 250 °C. Geochim. Cosmochim. Acta, 222, pp.130–145

Moore, E.K., Li, J., Zhang, A., Hao, J., Morrison, S.M., Hummer, D.R. and Yee, N. (2024). Uranium Redox and Deposition Transitions Embedded in Deep-Time Geochemical Models and Mineral Chemistry Networks. Geochemistry, Geophys. Geosystems, 25, p.e2023GC011267

Mudd, G.M. and Diesendorf, M. (2008). Sustainability of Uranium Mining and Milling: Toward Quantifying Resources and Eco-Efficiency. Environ. Sci. Technol., 42, pp.2624–2630

Muhling, J.R., Fletcher, I.R. and Rasmussen, B. (2012). Dating fluid flow and Mississippi Valley type base-metal mineralization in the Paleoproterozoic Earaheedy Basin, Western Australia. Precambrian Res., 212, pp.75–90

Ohmoto, H. and Goldhaber, M.B. (1997). Sulfur and carbon isotope. In: Barnes, H.L. (Ed.), Geochemistry of Hydrothermal Ore Deposits, 3rd edn. John Wiley and Sons, New York, pp.517–612

Pal, D.C., Barton, M.D. and Sarangi, A.K. (2009). Deciphering a multistage history affecting U–Cu(–Fe) mineralization in the Singhbhum Shear Zone, eastern India, using pyrite textures and compositions in the Turamdih U–Cu(–Fe) deposit. Miner. Depos., 44, pp.61–80

Pal, D.C., Das, E., Sasmal, A., Adak, S. and Abhinay, K. (2023). Role of evaporites in sodium metasomatism and formation of albite-rich rocks in IOCG provinces. Geochim. Cosmochim. Acta, 361, pp.210–227

Pal, D.C. and Rhede, D. (2013). Geochemistry and chemical dating of uraninite in the Jaduguda uranium deposit, Singhbhum shear zone, India-implications for uranium mineralization and geochemical evolution of uraninite. Econ. Geol., 108, pp.1499–1515

Pal, D.C., Trumbull, R.B. and Wiedenbeck, M. (2010). Chemical and boron isotope compositions of tourmaline from the Jaduguda U (–Cu–Fe) deposit, Singhbhum shear zone, India: Implications for the sources and evolution of mineralizing fluids. Chem. Geol., 277, pp.245–260

Patel, S. and Ozha, M.K. (2025). Geochemical evolution of uranium mineralization in the Mohuldih deposit, Singhbhum Shear Zone, India: constraints from uraninite and brannerite chemistry. Mineral. Petrol., 119, pp.105–125

Patel, S., Upadhyay, D., Mishra, B., Abhinay, K. and Sarangi, A.K. (2021). Multiple episodes of hydrothermal alteration and uranium mineralization in the Singhbhum Shear Zone, eastern India: constraints from chemical and boron isotope composition of tourmaline. Lithos 388–389, p.106084

Patel, S., Upadhyay, D., Ranjan, S. and Mishra, B. (2023). Magnetite-fluorapatite geochemistry and monazite U–Pb geochronology of the Mohuldih uranium deposit, Singhbhum Shear Zone, eastern India. Geol. J., 58, pp.2002–2027

Rasmussen, B., Fletcher, I.R. and Muhling, J.R. (2007). In situ U–Pb dating and element mapping of three generations of monazite: Unravelling cryptic tectonothermal events in low-grade terranes. Geochim. Cosmochim. Acta, 71, pp.670–690

Rasmussen, B., Fletcher, I.R., Muhling, J.R. and Wilde, S.A. (2010). In situ U–Th–Pb geochronology of monazite and xenotime from the Jack Hills belt: Implications for the age of deposition and metamorphism of Hadean zircons. Precambrian Res., 180, pp.26–46

Rich, R.A., Holland, H.D. and Petersen, U. (1977). Hydrothermal uranium deposits. Elsevier Applied Science.

Ridley, J. (2013). Ore deposit geology. Cambridge University Press.

Roedder, E. and Bodnar, R. (1997). Fluid inclusion studies of hydrothermal ore deposits. In: Barnes, H. (Ed.), Geochemistry of Hydrothermal Ore Deposits. John Wiley, New York, pp.657–698

Romberger, S.B. (1984). Transport and deposition of uranium in hydrothermal systems at temperatures up to 300 C: geological implications. In: Uranium Geochemistry, Mineralogy, Geology, Exploration and Resources. Springer, pp.12–17

Schidlowski, M., Eichmann, R. and Junge, C.E. (1975). Precambrian sedimentary carbonates: carbon and oxygen isotope geochemistry and implications for the terrestrial oxygen budget. Precambrian Res., 2, pp.1–69

Smith, D.K. (1984). Uranium mineralogy. In: De Vivo, B., Ippolito, F., Capaldi, G., Simpson, P. R. (Eds.), Uranium Geochemistry, Mineralogy, Geology, Exploration and Resources. The Institution of Mining and Metallurgy, London, England, pp.43–88. https://doi.org/10.1007/978-94-009-6060-2_6

Spirakis, C.S. (1996). The roles of organic matter in the formation of uranium deposits in sedimentary rocks. Ore Geol. Rev., 11, pp.53–69

Spirakis, C.S. (1981). The possible role of sulfate reduction kinetics in the formation of hydrothermal uranium deposits. Econ. Geol., 76, pp.2236–2239

Steiger, R.H. and Jäger, E. (1977). Subcommission on geochronology: Convention on the use of decay constants in geo- and cosmochronology. Earth Planet. Sci. Lett., 36, pp.359–362

Szalay, S. and Samsoni, Z. (1969). Investigation Of the Leaching of Uranium from Crushed Magmatic Rock. Geochem. Int., 6, pp.613-23

Taylor, H.P. (1997). Oxygen and hydrogen isotope relationships in hydrothermal mineral deposits. In: Barnes, H.L. (Ed.), Geochemistry of Hydrothermal Ore Deposits. Wiley and Sons, New York, pp.229–302

Timofeev, A., Migdisov, A.A., Williams-Jones, A.E., Roback, R., Nelson, A.T. and Xu, H. (2018). Uranium transport in acidic brines under reducing conditions. Nat. Commun., 9, p.1469

Vielreicher, N.M., Groves, D.I., Fletcher, I.R., McNaughton, N.J. and Rasmussen, B. (2003). Hydrothermal Monazite and Xenotime Geochronology: A New Direction for Precise Dating of Orogenic Gold Mineralization. SEG Discov., pp.1–16. https://doi.org/10.5382/SEGnews.2003-53.fea

Vielreicher, N.M., Groves, D.I., Snee, L.W., Fletcher, I.R. and McNaughton, N.J. (2010). Broad Synchroneity of Three Gold Mineralization Styles in the Kalgoorlie Gold Field: SHRIMP, U-Pb, and 40Ar/39Ar Geochronological Evidence. Econ. Geol., 105, pp.187–227

Wing, B.A., Ferry, J.M. and Harrison, T.M. (2003). Prograde destruction and formation of monazite and allanite during contact and regional metamorphism of pelites: petrology and geochronology. Contrib. to Mineral. Petrol., 145, pp.228–250

Wood, S.A. and Ricketts, A. (2000). Allanite-(Ce) from the Eocene Casto granite, Idaho: Response to hydrothermal alteration. Can. Mineral., 38, pp.81–100

Xing, Y., Mei, Y., Etschmann, B., Liu, W. and Brugger, J. (2018). Uranium Transport in F-Cl-Bearing Fluids and Hydrothermal Upgrading of U-Cu Ores in IOCG Deposits. Geofluids, 2018, p.6835346. https://doi.org/10.1155/2018/6835346

Zack, T., Stockli, D.F., Luvizotto, G.L., Barth, M.G., Belousova, E., Wolfe, M.R. and Hinton, R.W. (2011). In situ U–Pb rutile dating by LA-ICP-MS: 208Pb correction and prospects for geological applications. Contrib. to Mineral. Petrol., 162, pp.515–530

